

Investigations of Modified Functional Connectivity at Rest in Drug-Resistant Temporal Lobe Epilepsy Patients

Deepa Nath¹, Dr. Anil Hiwale², Dr. Nilesh Kurwale³, Dr.C.Y.Patil⁴
School of ECE, Dr.Vishwanath Karad MIT World Peace University, Pune^{1,2}
Neurosurgeon, Deenanath Mangeshkar Hospital, Pune³
Dept of Instrumentation and Control, COEP Technological University, Pune⁴

Abstract—In this experimental study patients with temporal lobe epilepsy and controls have been compared for functional connectivity (FC) using resting-state functional magnetic resonance imaging (rs-fMRI). This research work examines the alterations to better understand the issues with brain activity of individuals suffering from Temporal Lobe epilepsy (TLE), during the rest state. The major objective of this study is to investigate FC-related alterations in the resting state to fully comprehend the complex nature of epilepsy. It is observed that FC gets altered in specific regions in the case of patients suffering from left-sided Temporal Lobe Epilepsy and right-sided Temporal Lobe Epilepsy as compared to controls. Using rs-fMRI, it is found that the right-sided TLE patient group had altered hippocampus networks than the control right-side group. There are considerable differences between the left and right areas of control and the groups with mesial temporal hippocampal sclerosis on the left and right sides. When compared to control left brain regions, the left-side TLE group exhibits reduced connection between the anterior cingulate gyrus and the affected hippocampus and increased regional connectivity between the affected hippocampus and the default posterior cingulate cortex region.

Keywords—Temporal Lobe Epilepsy (TLE); resting-state Functional Magnetic Resonance Imaging (rs-fMRI); Functional Connectivity (FC); Blood Oxygen Level-Dependent (BOLD)

I. INTRODUCTION

Over the past few years, resting-state Functional Magnetic Resonance Imaging, (rs-fMRI), has been used. The rs-fMRI studies of the human connectome have gained popularity, and these studies are extremely valuable for understanding epilepsy networks and improving surgical treatment. Surgery to remove epileptogenic tissues may be a successful course of treatment for 20– 30% of epilepsy patients whose seizures are unresponsive to medication [1]. The most successful method for treating drug-resistant epilepsy is surgery. After thorough presurgical evaluation, seizure freedom can be achieved in approximately 60- 70% of patients [2].

FC of a brain network explains the patterns and degree of temporal correlations of activation patterns across distant brain regions. FC is a metric for the understanding relationship between different brain areas. A significant portion of the current work is based on assumptions regarding which parts of the brain are active when it is at rest. This calls

for monitoring the relative changes of Blood Oxygenated level-dependent (BOLD) signal in comparison to the baseline in different brain regions when it is at rest [3]. Emerging neuroimaging research generally supports the idea that resting-state BOLD variations are at least largely caused by intrinsic brain activity [4, 5]. Consequently, investigations on spontaneous regional interactions happen when the brain is at rest. Epilepsy in the mesial temporal lobe (MTLE) is studied extensively for clinical characteristics and neuropsychological deficits [6, 7].

TLE is associated with various neuropsychological deficits beyond the boundaries of the temporal lobe and apart from memory; other common deficits associated with TLE include the domains of executive function, language, and cognition [4]. Right and left TLE presents visual and verbal memory deficit profiles, which were traditionally used for lateralizing the epileptogenic lesion however; overall neuropsychological deficits were more common with left TLE patients [4]. Moreover, the dominance of the lobe is known to affect the pattern of neuropsychological deficits but the extent of deficits always remains unpredictable.

However, the right and left TLE differ in language, executive function, and social cognition, according to neuropsychological literature on TLE, which is the clinical expression of functional connection. The work presented in the paper aims to examine the variations in resting-state connection networks in well-matched cohorts of patients with right- and left-sided TLE and to compare them to healthy controls in the respective regions of the right and left brain.

Low-frequency neural oscillations have been the subject of novel rs-fMRI research [5] that has progressed in the neuroscience literature. [3,4]. Functional connections of various brain regions using rs-fMRI help explain TLE's neuropsychological deficits [6, 7, and 8]. Most of the methods of the rs-fMRI utilize group analysis using various algorithms and pipelines [9] where different preprocessing steps are applied and signals are averaged for the group and plotted.

Numerous epilepsy network investigation studies [10, 11, and 12] have examined groups with left and right-side involvement. In several studies, the Left TLE (LTLE) or Right TLE (RTLE) is compared to the Healthy Control group. The unique feature of this experiment is that regions related to the

right-side memory circuits of the Control and the right-side TLE groups are compared, and comparable comparisons were made for the left-side group. The functional connectivity between regions of interest (ROI) inside and outside the epileptogenic network was assessed in the right or left regions of patients with treatment-resistant RTLE or LTLE and control participants, respectively. The introduction is mentioned in Section I, the dataset and methods are described in Section II, analysis and results obtained during experimentation are discussed in Section III, the results obtained and their comparison to the work of other researchers are discussed in Section IV, the limitations and future directions of the study are discussed in Section V, and the conclusion is stated in Section VI.

II. MATERIAL AND METHODS

A. Study Period

MRI data collection for patients and controls was done for the period of the past two years from 2021 to year 2022.

TABLE I. SUBJECT-SPECIFIC DEMOGRAPHIC DATA

Subjects	Controls	LTLE	RTLE
N (Male, Female)	16 (15, 1)	9 (5, 4)	7(5, 2)
Mean age (years)	20.83	20.87	26.14
Epilepsy Duration in years(mean±SD)		8.85±5.87	14.85±13.04
Antiepileptic Drugs(AED) (mean±SD)		2.57±0.53	3±0.69
Seizure frequency/month(mean±SD)		1.6±1.54	1.16±0.408

D. MRI Data Acquisition Parameters

1) *Patient conditioning*: Before the start of the resting state acquisition, patients were advised to recline comfortably with their eyes closed as the regular epilepsy surgery scanning was conducted on a single scanner.

2) *Structural T1 data*: High-resolution structural data which is used to quantify brain structure sequence was acquired in 256x256 matrix, 3D acquisition without any gap with a slice thickness =0.5 mm, echo time = 3.07ms, Repetition time (TR) = 3000 ms, and flip angle= 8° with voxel size was 0.5x0.5x0.5 mm

3) *Functional data*: It is employed to research brain activity. BOLD data was acquired in a one-shot gradient echo-planar imaging sequence with parameters in a single direction. A total of seven minutes and 140 volumes of a sequence were recorded using a flip angle of 90 degrees, a repetition time of 3000 ms, and an echo time (TE) of 30 ms.

E. Imaging

With the aid of a 3T MRI system (Siemens), imaging was carried out. The following settings were used for functional imaging: repetition time (TR) = 3000 msec, echo time (TE) =30 msec, slice thickness = 2 mm, and 36 slices. The same imaging investigation produced high-resolution structural pictures. fMRI recordings, each lasting seven minutes, were made during the imaging sessions.

F. Pre-processing

Regions of interest (ROI) default for 164 regions were created from T1 scans in the CONN toolbox [13] and used

B. Participants

Patients with temporal lobe epilepsy who are drug-resistant, with unilateral hippocampal scleroses that were deemed candidates for standard anterior temporal lobectomy and amygdalo hippocampectomy formed the patient group. All the patients had the scans on a single magnetic resonance imaging Siemens make 3T MRI scanner (Skyra). Left and right TLE groups of patients were separated. Separately data was generated for the control group. Our study sample includes right TLE (n=07), left TLE (n=09), and controls (n=16), which makes a total of 32 participants. Demographic data is mentioned in Table I.

C. Ethical Standards

The present study is approved by the Independent Institutional Review Board (IRB) for all the components of the study. All the ethical practices have been followed while the study is been carried out. Informed consent was taken from all participants.

Harvard-Oxford Atlas [14]. All volumes were segmented, and normalized, slice time was adjusted, co-registered to T1, and realigned to the first functional scan using the Montreal Neurological Institute (MNI) 152 template.

The head movement artifacts are eliminated, high-pass filtering is applied for 100 s, and spatial smoothing is performed at 8 mm full-width half-maximum. The SPM12 (statistical parametric mapping) is used for preliminary data processing for each patient. The procedures for realignment and slice-time adjustment are standard and CONN uses the Artifact Detection Tools (ART) to look for outliers. Direct normalization in [15] is the method we choose to utilize to normalize the standard template of MNI152 space. After performing structural segmentation and normalization, the BOLD signal-to-noise ratio is then improved using a Gaussian kernel with an 8mm full width at half maximum(FWHM).

G. Denoising

Physiological, head-motion and other sources of noise must be reduced to focus on low-frequency oscillations while reducing their overall volume, BOLD data are filtered in the temporal domain using a band-pass filter of 0.008 to 0.9 Hz before further processing. To decrease the influence of variation of FC values is measured between pairs of randomly selected ROIs in the brain to gauge the effectiveness of the procedure (see Fig. 1 for a specific Subject 1).

H. First-Level Analyses

To describe the functional connectivity between each pair of areas, ROI-to-ROI connectivity (RRC) matrices [16] were calculated. The correlation coefficient's sample distribution, or Pearson's r, can be transformed into a normally

distributed distribution using the Fisher Z-Transformation. The level of functional connectivity is measured using Fisher-transformed bivariate correlation coefficients from a general linear model (weighted-GLM) [17], as stated in (1) which were independently computed for each pair of ROIs and characterized the relationship between their BOLD signal time series. Refer to Fig. 2 for the first-level analyses.

The analyses for this study examined the ROI-to-ROI connections between brain regions for memory circuits. It is limited to a particular set of 12*12 connections (refer to Table

II) out of all available connections (164x164). The degree of connectivity between each pair of ROIs among a pre-defined region RRC. Using this selected list of ROI, as described in Table II, an investigation for individual differences was carried out for RTLE, LTLE, and controls.

$$r(i, j) = \frac{\int R_i(t)dt R_j(t)dt}{\int (R_i^2(t)dt R_j^2(t)dt)^{1/2}} \quad (1)$$

$$Z(i, j) = \tan h^{-1}(r(i, j)) \quad (2)$$

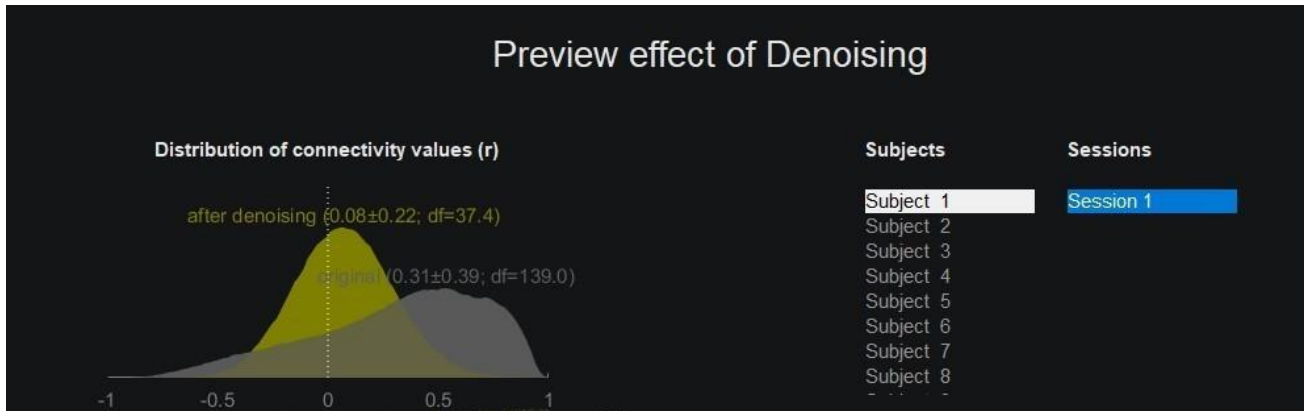


Fig. 1. Denoising effect for a particular subject.

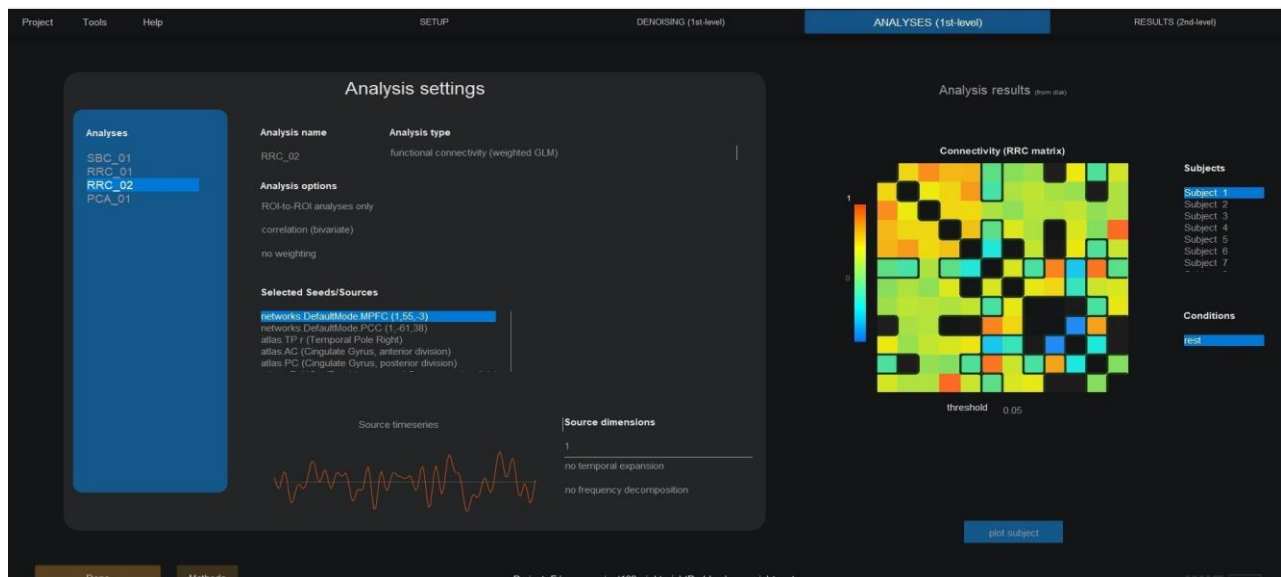


Fig. 2. First level analysis GUI display on CONN toolbox [16].

where R is the BOLD time series inside each ROI, Z is the RRC matrix of Fisher-transformed correlation coefficients, r is a matrix of correlation coefficients (see (2)), and Z is the matrix of Fisher-transformed correlation coefficients (all-time series are assumed to be centered to zero mean here for simplicity). In the first level of analysis we need to choose the method of connectivity like Seed-based connection (SBC) or Region Region Connectivity (RRC), Principal Component Analysis, and many more. For this study, 12 ROIs are compared for connectivity analysis as listed in Table II. As a result, connectome rings appear on the

CONN Graphical User Interface (GUI), and the variations between them were quantified visually.

I. Group/Second Level Analysis

Second-level analyses are used to draw conclusions about the characteristics of groups or populations. CONN uses the General Linear Model (GLM) [17] to examine functional connectivity data at the second level.

Selecting one or more items from the “Subject effects” list and indicating the desired 'between-subjects contrast' establishes a second-level model in CONN. Control and

Patients are the two groups designated in this experiment, and they are originally listed in the covariates tab during setup and enter [1 -1] to evaluate the differences between the groups ‘connections. Otherwise, just enter [1 0] or [0 1] and refer to Fig. 3 in the ‘Between-Subject Contrast’ to understand the individual effects of Controls or Patients independently. The evaluation of the connection-level hypothesis uses multivariate parametric statistics with random effects across participants and sample covariance estimates across different data. The inferences were analyzed on a per-cluster basis (groups of linked connections). Based on parametric statistics between and within each pair of network-level identifiers as independent variables, cluster-level inferences were made. Refer to Fig. 3 for Second Level Analysis. Functional Network Connectivity [13], which employs complete-linkage hierarchical clustering and the ROI-to-ROI physical closeness and functional similarity metrics [16], to discover networks. Results were threshold using a family-wise adjusted p-FDR= 0.05 cluster-level Threshold [18] in addition to a p= 0.05 connection-level threshold [19].The results of the first-level studies of each individual are combined at this stage to analyze the total population. When conducting group-level analysis, the effect estimates of the General Linear Model are frequently combined across participants using the t-test, ANOVA, ANCOVA, multiple regression, or linear mixed-effects (LME) models. The subject-effects (X), conditions (Y),

between-subjects contrast (C), and between-conditions contrast (M) matrices are the only ones that must be specified for the GLM framework. As a result, the same GLM framework can be used to specify a very wide range of traditional analyses.

TABLE II. SELECTED ROI FOR COMPARISON WITH RTLE, LTLE, AND CONTROLS

Sr.No	Region of Interest	Abbreviations
1.	Default Mode.The medial prefrontal cortex (MPFC)	MPFC
2.	DefaultMode.Posterior cingulate cortex(PCC)	PCC
3.	Temporal Pole affected	TP r/l
4.	Cingulate Gyrus, anterior division	AC
5.	Cingulate Gyrus, posterior division	PC
6.	Parahippocampal Gyrus, anterior division affected	aPaHC
7.	Parahippocampal Gyrus, posterior division affected	pPaHC
8.	Planum Temporal affected	PT r/l
9.	Hippocampus affected	Hippo r
10.	Hippocampus contralateral	Hippo l
11.	Amygdala affected	Amy r/l
12.	Insular Cortex affected	IC r/l

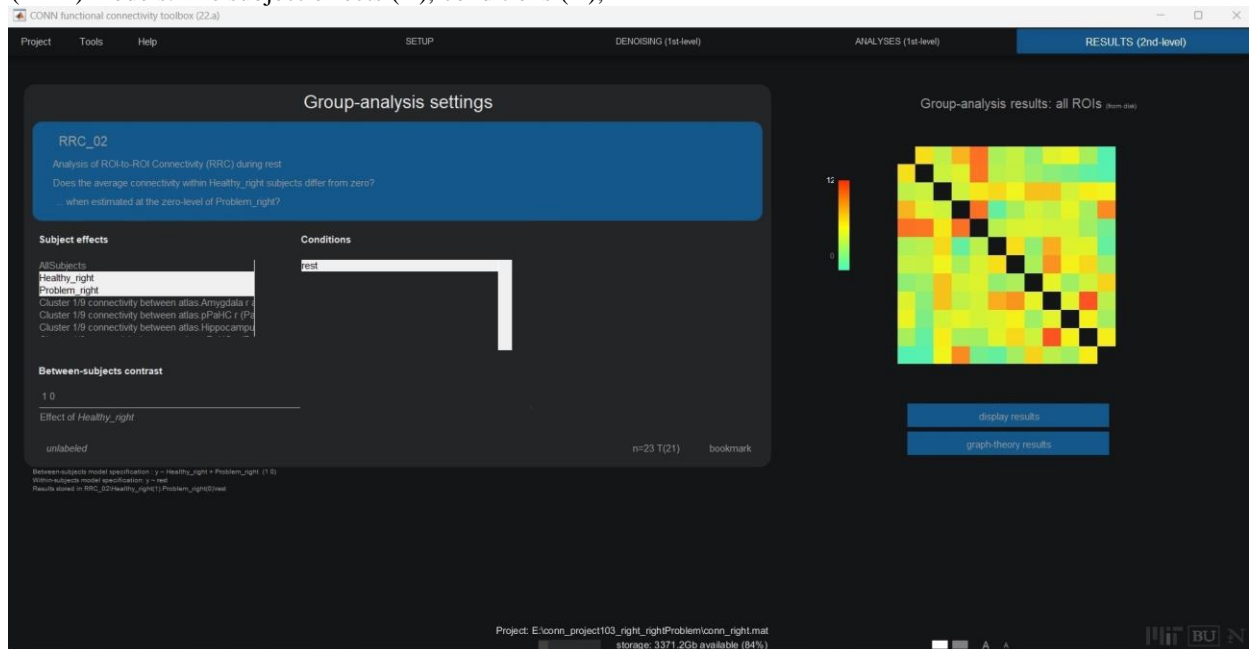


Fig. 3. Second-level analysis for group level [16].

III. ANALYSIS AND RESULTS

The analysis is performed on the CONN toolbox, 2022a [13], an SPM-based toolbox that runs on MATLAB 2022a. Two groups were used for the intergroup comparisons: Healthy_l controls for the left side regions of the brain with patients who had LTLE, and Healthy_r controls for the right side parts of the brain with patients who had RTLE. To further investigate the results, all the data is plotted on connectome rings and brain templates. Default Color coding is used to

interpret the connection strength, from the blue to red spectrum where blue is negative and red is an extremely positive correlation or connectivity amongst the ROIs. The second-level results tab of CONN generates a ROI.mat file after processing the images. The intriguing results in this file can be used to draw a conclusion. Here, names provide a list of ROI sources, h value provides the Fisher transformed correlation value based on the particular contrast used during the experiment, F values show the value of the statistic, and P values provide one-sided tail values.

The ROI.mat files produced during the second level analysis can be used to generate graphical results visualization in CONN GUI. Ring Connectome results for the ROI to ROI connections as specified in Table II are displayed. Both graphical visualizations of group-level analysis are compared with the help of ring connection display and RRC matrix.

The data displayed on the ring connectome is as shown in Fig. 4. The 3D brain view displayed in Fig. 5 can be viewed in the same Conn GUI. As shown in Fig. 4, there are apparent differences in the correlation values between Healthy_r and other ROI in the RTLE group. As seen in Fig. 5, the medial prefrontal cortex (MPFC) and posterior cingulate cortex (PCC), two of the default mode networks with the contralateral hippocampus, are no longer connected to one another. Also in the RTLE group, the amygdala and hippocampus both lack connections to the anterior cingulate and PCC regions, respectively. The RRC matrix, which is accessible through the CONN GUI, only outputs color variations between various pairs of ROI. With the help of Python code and the h, F, or P values from the ROI.Mat file, distinct RRC matrices can be produced. Here, the RRC matrix is made using h values, and the correlation values are displayed in the boxes for comparison between the affected RTLE patients and the control group (see Fig. 6).

The 12 interest ROIs are taken into account (see Table II). Additionally, two sample t-tests were run in the second-level analysis to compare the Controls and RTLE groups. In the results explorer GUI's customize menu, under the advanced Family Wise Control Settings, the connectivity threshold set to $p < 0.05$ and cluster threshold $p < 0.1$, as shown in Table III.

A plot of Effect Size is displayed in Fig. 7 about clusters of interest. Effect size is the measure of connection, which is commonly shown by Fisher-transformed correlations. From Fig. 7, the default mode posterior cingulate cortex (PCC) connectivity to the impacted Planum Temporal differs between the right TLE and the healthy control right areas of the brain. While this connection is absent in the control right-side memory network regions, significant connectivity between these anterior parahippocampal regions and the temporal pole is observed in RTLE.

TABLE III. DIFFERENCES IN CONNECTIVITY VALUES

Sr.No	ROI Region connections	Tstat, p-value
1	ROI 1/12 PCC to PTr	3.16,p=0.004
2	ROI 3/12 PC -AC	2.89,p=0.008
3	ROI 3/12 Hippo-left -AC	2.39,p=0.02
4	ROI 3/12 PC-PTr	2.39,p=0.02
5	ROI 3/12 aPaHC-PTr	-2.40,p=0.02

Similar to this, functional connectivity was compared between the Healthy Left Controls and the LTLE patient group. The results displayed on the ring connectome in Fig. 8 can also be viewed in a 3D brain perspective using the same Conn GUI. From Fig. 9, visually what can be observed is in the control group left all the selected ROIs are connected with other ROIs, whereas in the LTLE group, the connections with other ROIs are altered, prominently default

mode networks like medial prefrontal cortex (MPFC) and Posterior Cingulate Cortex (PCC) have connectivity with the affected temporal pole (TP1) and affected Planum Temporal (PT 1). Also, the AffectedHippocampus is not connected with the Anterior Cingulate Gyrus. The correlation values heat map is plotted as shown in Fig. 10 for comparing Healthy left side regions of the brain with the LTLE patient group based on correlation values. In addition, by selecting Subject Effects as both Healthy l and LTLE groups in Second Level Analyses, we attempted to do a two-sample T-Test for the comparison within two groups Healthy left side regions of the brain and LTLE impacted group. Similar settings were used like the right side comparison. A plot of Effect size referred to Fig. 11 concerning clusters of interest is shown. Effect size -is the magnitude of connectivity typically Fisher transformed correlations are displayed. Refer to Table IV for Connectivity differences, Fig. 11, the differences observed are listed.

TABLE IV. CONNECTIVITY DIFFERENCES

Sr.No	ROI	Region	Tstat, p-value
1	ROI 2/12	PCC to AC	2.47,p=0.02
2	ROI 2/12	Left Hippocampus -AC	2.30,p=0.03

Differences noted in this intergroup comparison are when compared to the Healthy Control left side regions to the left TLE's- default mode network (PCC) connectivity to the Cingulate Gyrus' anterior division is noticeably different. Also when compared to healthy control left regions the connectivity of the affected hippocampus region with the Anterior Cingulate Gyrus (AC) dramatically diminished in LTLE.

IV. DISCUSSION

A. Alterations Observed in the RTLE Group with Control Right Regions

The results of the experiment as shown Fig. 6 reveal that RTLE patients showed less connection between the affected Planum Temporal, affected Hippocampus, and contralateral Hippocampus with Default Mode MPFC area. Also, it was discovered that the Planum Temporal and Affected Hippocampus in the RTLE group exhibited decreased connection for the Default mode PCC region. Additionally, RTLE revealed a weakening of the connection between the anterior division of the cingulate gyrus and the contralateral hippocampus. Also, the posterior cingulate gyrus showed a weaker connection with the contralateral hippocampus.

B. Alterations Observed in the LTLE Group with Control Left Regions

With reference to Fig. 10, it is observed that there is a weak link between the afflicted hippocampus and the Amygdala with the default mode MPFC when LTLE patients were compared to groups of healthy control left region. Also discovered that in LTLE group anterior cingulate gyrus has a decreased connectivity with the affected hippocampus. A stronger link between the injured and contralateral hippocampi and the PCC in default mode was also seen. A weakened connection between the Planum Temporal affected with Amygdala is observed in LTLE as compared to the control group.

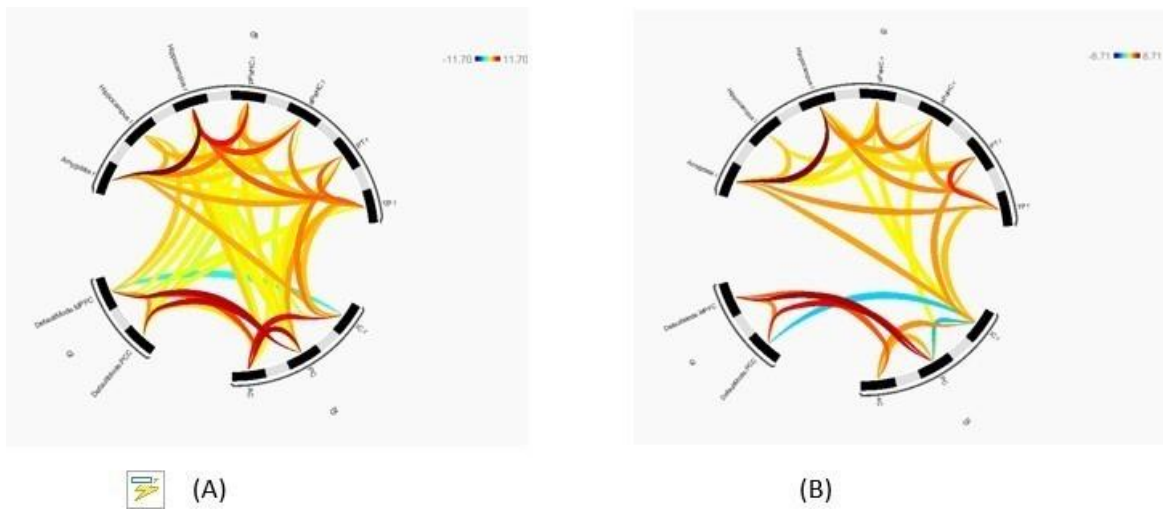


Fig. 4. Ring connectome comparison (A) Healthy_r with (B) RTLE.

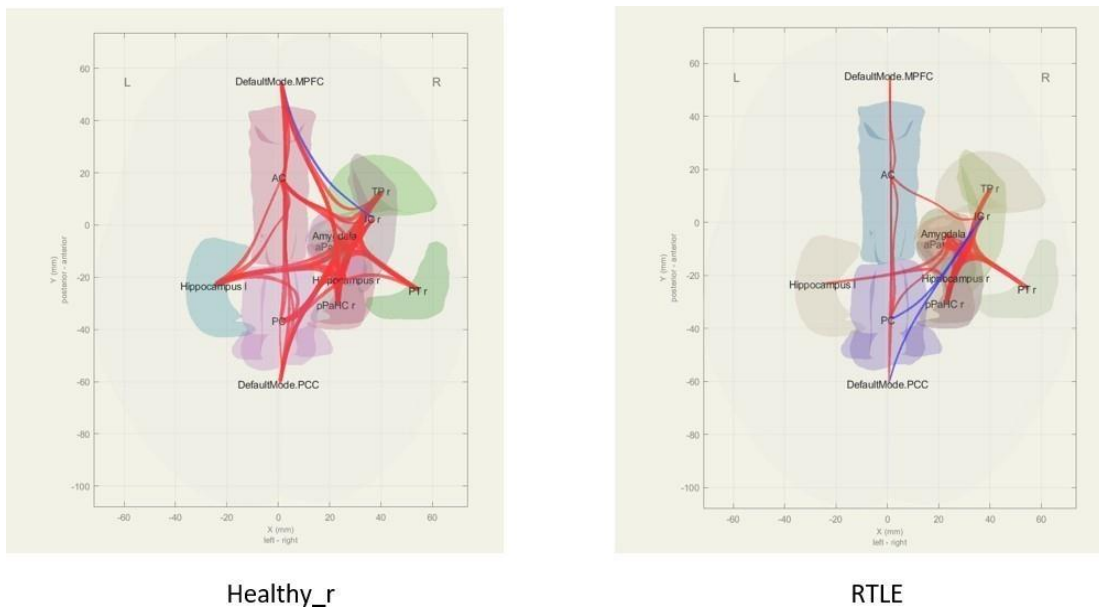


Fig. 5. Healthy_r versus RTLE results on 3D brain view.

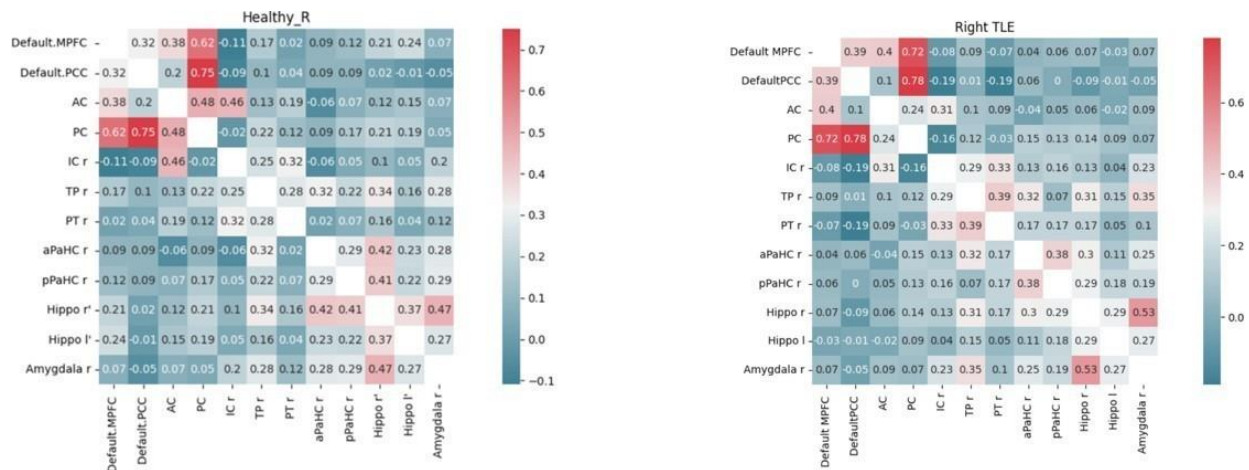


Fig. 6. Correlation values for healthy versus RTLE matrix values display. Heatmap is created based on fisher transformed correlation coefficient based on python version 3.10.



Fig. 7. Plot Effects –average effect sizes with the selected clusters.

C. A Few Relevant Case Studies

Haneef et al. [20] in their study of LTLE 13 patients, RTLE 11 patients, and 16 healthy controls also report similar findings, wherein Default mode connectivity gets more affected in TLE patients, Default mode Network with the hippocampi. Pierera et al. [21] in their study of ROI-ROI analysis of 18 patients and nine healthy controls report asymmetrical loss of connectivity between left and right Hippocampus Sclerosis in a similar fashion but the authors only studied hippocampal seed, unlike our study where all the other important connectivity profiles like DMN and memory networks are also explored.

In a study by Zhao, [22] involving 12 LTLE patients, 11 RTLE patients, and 23 healthy controls, functional connectivity differences were examined using ROI- based analysis. In this study, the LTLE group had a significantly lower link with the anterior and posterior parahippocampus gyrus compared to the controls. The reduced connection between areas in the bilateral temporal lobes and frontal lobes was also discovered on the right side. Pressl [23] et al. used rs-fMRI to investigate a potential link between TLE treatment response and functional network alterations. In individuals with treatment-resistant and well-controlled epilepsy, they looked at variations in functional connectivity between regions of interest (ROI) inside and outside the epileptogenic network. As suggested in their findings the thalamo-hippocampus positively correlated in Controls, while they are negatively correlated in treatment resistance TLE patients and this could serve as a new biomarker for TLE diagnosis and preventive

treatment. In another study of Marine Fleury [24] where 43 controls and 29 TLE patients connectivity was studied, Patients with TLE had enhanced regional connectivity between the anterior Mesial Temporal Lobes (MTL) on both sides and widespread decreased connectivity between the frontal lobes and MTLs as compared to controls.

Another study by Barnett [25] found that in persons with temporal lobe epilepsy (TLE), the hippocampus's connections to other parts of the default mode network (DMN) are a reliable predictor of memory function. Using resting state fMRI data from individuals with left-sided TLE (LTLE) and right-sided TLE (RTLE), they divided the hippocampus based on its functional links to the rest of the brain, as well as from a set of neurologically healthy controls. Other Default mode Networks (DMN) regions are less connected to the medial prefrontal cortex (mPFC) and posterior cingulate cortex (PCC), two important sections of the DMN, were reduced in both TLE groups. The anterior region of the hippocampus in the LTLE group also displayed a decreased connection to the DMN. This is in line with the findings made in this experiment, which showed that the hippocampus-to-DMN connection can be used as a helpful marker for persons who have temporal lobe epilepsy. Future research will be useful in determining whether anterior and posterior biases in connection are associated with the impairment of more precise memory functions in TLE patients. The importance of these findings can also be understood with the use of clinical neuropsychology correlation. Here in this study for memory circuits, a selected group of ROI was chosen for analyses. This list of ROI can vary for different network studies.

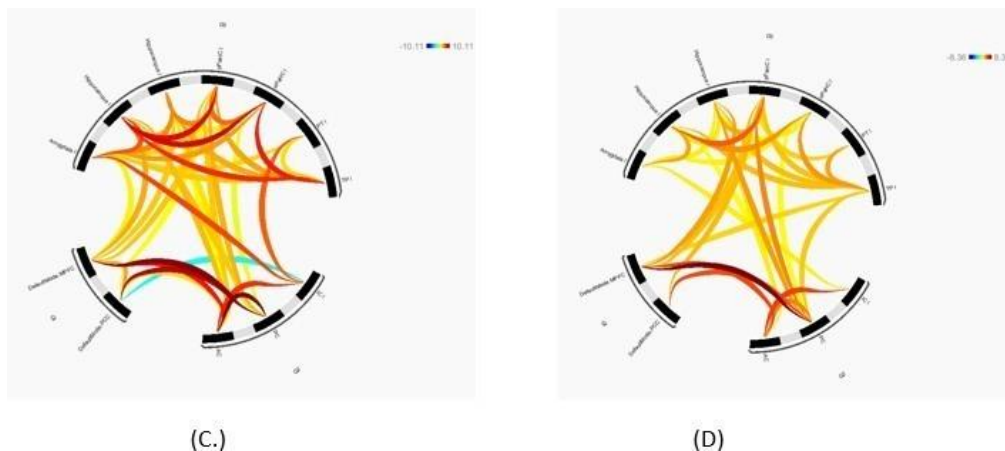


Fig. 8. Ring connectome comparison (C) Healthy_1 with (D) LTLE.

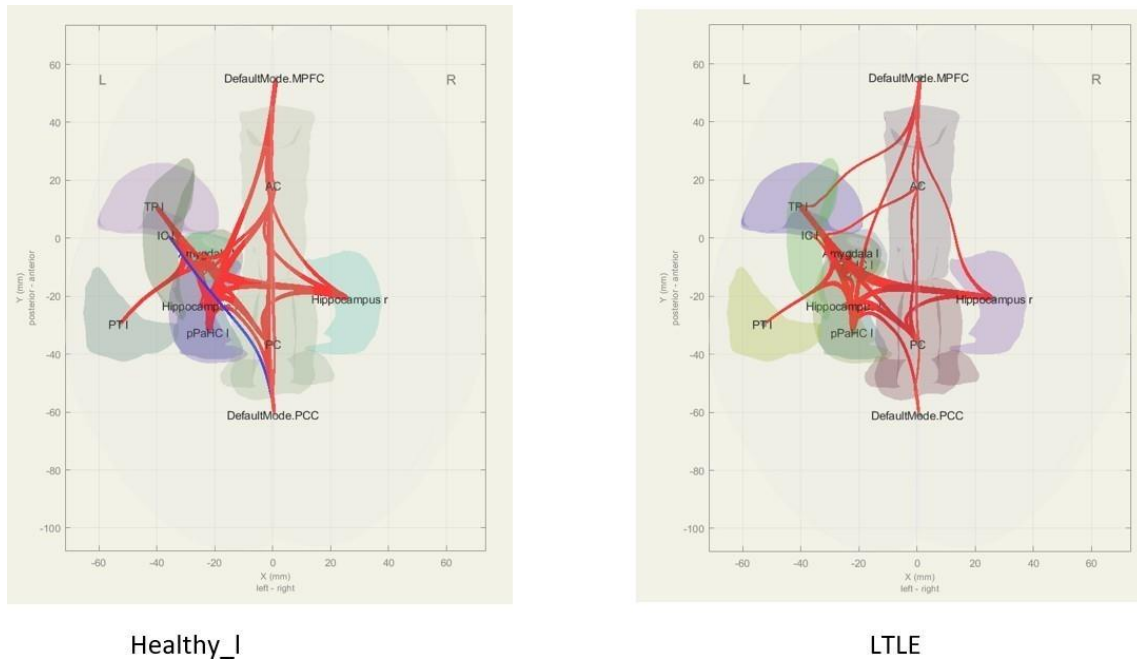


Fig. 9. Healthy_1 versus LTLE results on 3D brain view.

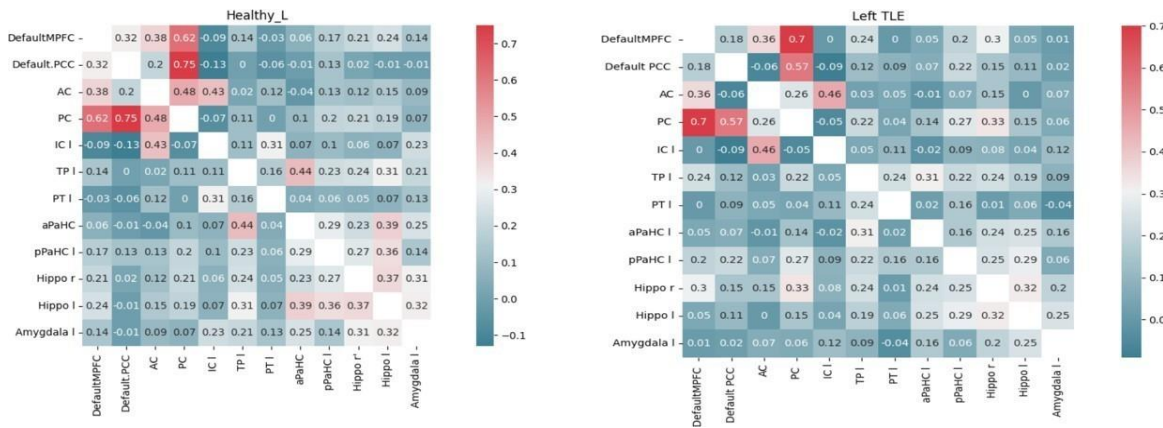


Fig. 10. Correlation values for healthy versus LTLE matrix values display. A heat map is created based on Fisher transformed correlation coefficient.

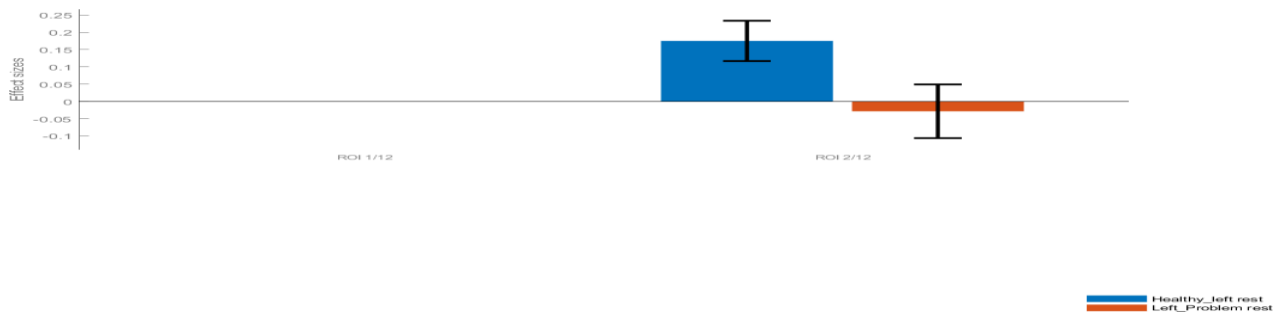


Fig. 11. Plot Effects—average effect sizes with the selected clusters.

V. LIMITATIONS AND FUTURE SCOPE

It is not that easy to generate the data for healthy subjects. In this study, data of 16 healthy controls was arranged with proper consent from the volunteers; however, a larger sample size may increase the accuracy of the analysis. The larger dataset may help to validate the variations in connections that

are clinically relevant and correlated. It will help to characterize TLE patients and provide more information about neurologic abnormalities. Also with different sets of ROI selections, it can be expanded for attention, language, visual, motor, sensory networks, and many other networks of the brain.

VI. CONCLUSION

The distinguishing feature of this experimental study is the comparison of right-side memory circuit-related regions of the control group with that of the right-side TLE group as well as the comparison of the left-side memory circuit-related regions of the control group with that of the left-sided TLE group. The mesial temporal hippocampus sclerosis patient group on the left and right sides exhibit distinct changes in the organization of the memory networks in comparison with the control group left and right sides. By comparing the RTLE patient group to the right-side Control group, the differences have been identified in the hippocampal network. The two default mode networks MPFC and PCC have weaker connectivity between the affected and contralateral hippocampi. In the LTLE patient group, reduced connections have been observed for impacted Planum Temporal and Default MPFC. Comparing LTLE to the control group for left brain areas, it has been observed that there was a decreased connection between the anterior cingulate gyrus and the affected hippocampus and more connectivity between the affected hippocampus and the default posterior cingulate cortex.

REFERENCES

- [1] C. Zhang and P. Kwan, "The Concept of Drug-Resistant Epileptogenic Zone", *Frontiers in Neurology*, Volume 10, pp. 558–558, 2019.
- [2] J.-A. Witt, T. Krutenko, M. Ga'deke, R. Surges, C. E. Elger, and C. Helmstaedter, "Accuracy of expert predictions of seizure freedom after epilepsy surgery," *Seizure*, vol. 70, pp. 59–62, 2019.
- [3] K. A. Smitha, K. Raja, K. M. Arun, P. G. Rajesh, B. Thomas, T. R. Kapilamoorthy, and C. Kesavadas, "Resting-state fMRI: A review on methods in resting state connectivity analysis and resting state networks," *Neuro-radiology J*, vol. 30, no. 4, pp. 5 524 274–5 524 274, 2017.
- [4] H. Lv, Z. Wang, E. Tong, L. M. Williams, G. Zaharchuk, M. Zeineh, A. N. Goldstein-Piekarski, T. M. Ball, C. Liao, and M. Wintermark, "Resting-State Functional MRI: Everything That Nonexperts Have Always Wanted to Know," *American Journal of Neuroradiology*, vol. 39, no. 8, pp. 1390–1399, 2018.
- [5] B. Biswal, F. Z. Yetkin, V. M. Haughton, and J. S. Hyde, "Functional connectivity in the motor cortex of resting human brain using echoplanar MRI," *Magn Reson Med*, vol. 34, no. 4, pp. 537–578, 1995.
- [6] W. Liao, Z. Zhang, Z. Pan, D. Mantini, J. Ding, X. Duan, C. Luo, Z. Wang, Q. Tan, G. Lu, H. and C, "Default mode network abnormalities in mesial temporal lobe epilepsy: a study combining fMRI and DTI," *Hum Brain Mapp*, vol. 32, no. 6, pp. 883–95, 2011
- [7] Cataldi M, Avoli M, de Villers-Sidani E. "Resting-state networks in temporal lobe epilepsy", *Epilepsia*. 2013 Dec;54(12):2048-59.
- [8] A. Barnett, S. Audrain, and M. P. Mcandrews, "Applications of Resting-State Functional MRI Imaging to Epilepsy," *Neuroimaging Clin N Am*, vol. 27, no. 4, pp. 697–708, 2017.
- [9] D. Nath, A. Hiwale, and N. Kurwale, "Optimization of Pipeline through Preprocessing Steps Sequence Alteration using Graph Theory for Resting-State fMRI," *International Journal of Engineering Trends and Technology*, vol. 71, no. 3, pp. 168–174, 2023.
- [10] C. Fu, A. Aisikaer, Z. Chen, Q. Yu, J. Yin, Yang, and W, "", Different Functional Network Connectivity Patterns in Epilepsy: A Rest-State fMRI Study on Mesial Temporal Lobe Epilepsy and Benign Epilepsy with Centrotemporal Spike," *Front Neurol*, vol. 12, pp. 668– 856 ,2021.
- [11] J. Royer, S. Bernhardt, E. Bc, Larivie`re, Gleicherrcht, S. Vorderwu`lbecke, Bj, and Vullie`moz, "Epilepsy and brain network hubs," *Epilepsia*, vol. 63, pp. 537–550, 2022.
- [12] M. Centeno and D. W. Carmichael, "Network Connectivity in Epilepsy: Resting State fMRI and EEG-fMRI Contributions," *Front Neurol*, vol. 5, pp. 93–93, 2014.
- [13] Nieto-Castanon, A. (2020b). 'fMRI minimal preprocessing pipeline'. Handbook of functional connectivity Magnetic Resonance Imaging methods in CONN, pages 3–16.
- [14] R. S. Desikan, F. Se'gonne, B. Fischl, B. T. Quinn, B. C. Dickerson, D. Blacker, R. L. Buckner, A. M. Dale, R. P. Maguire, B. T. Hyman, M. S. Albert, and R. J. Killiany, "" An automated labeling system for subdividing the human cerebral cortex on MRI scans into gyral based regions of interest," *Neuroimage*, vol. 31, no. 3, pp. 968–980, 2006.
- [15] V. D. Calhoun, T. D. Wager, A. Krishnan, K. S. Rosch, K. E. Seymour, M. B. Nebel, S. H. Mostofsky, S. H. Nyalakanai, P. Kiehl, and K, "The impact of T1 versus EPI spatial normalization templates for fMRI data analyses," *Hum Brain Mapp*, vol. 38, no. 11, pp. 5331–5342, 2017.
- [16] Nieto-Castanon, A. (2020c). 'fMRI minimal preprocessing pipeline'. Handbook of functional connectivity Magnetic Resonance Imaging methods in CONN, pages 26–62
- [17] Nieto-Castanon, A. (2020d). 'General Linear Model'. Handbook of functional connectivity Magnetic Resonance Imaging methods in CONN, pages 63–82.
- [18] Nieto-Castanon, A. (2020a). 'Cluster-level inferences'. Handbook of functional connectivity Magnetic Resonance Imaging methods in CONN, pages 83–104
- [19] Y. Benjamini and Y. Hochberg, ""Controlling the false discovery rate: a practical and powerful approach to multiple testing," *Journal of the Royal Statistical Society: series B (Methodological)*, vol. 57, no. 1, pp. 289–300, 1995.
- [20] Z. Haneef, A. Lenartowicz, H. J. Yeh, H. S. Levin, J. E. Jr, and J. M. Stern, "JM. 'Functional connectivity of hippocampal networks in temporal lobe epilepsy,'" *Epilepsia*, vol. 55, no. 1, pp. 137–182, 2014.
- [21] F. R. Pereira, A. Alessio, and M. S. Sercheli, ""Asymmetrical hippocampal connectivity in mesial temporal lobe epilepsy: evidence from resting state fMRI," *BMC Neuroscience*, vol. 11, pp. 66–66, 2010.
- [22] X. Zhao, Z. Q. Zhou, Y. Xiong, X. Chen, K. Xu, J. Li, Y. Hu, X. L. Peng, and W. Z. Zhu, "Interhemispheric White Matter Asymmetries in Medial Temporal Lobe Epilepsy With Hippocampal Sclerosis," *Frontiers in Neurology*, vol. 10, pp. 394–394, 2019.
- [23] C. Pressl, P. Brandner, S. Schaffelhofer, K. Black- mon, P. Dugan, M. Holmes, T. Thesen, R. Kuzniecky, O. Devinsky, and W. A. Freiwald, "Resting-state functional connectivity patterns associated with pharmacological treatment resistance in temporal lobe epilepsy," *Epilepsy Research*, 2019.
- [24] M. Fleury, S. Buck, L. P. Binding, L. Caciagli, S. B. Vos, G. P. Winston, P. J. Thompson, M. J. Koeppe, J. S. Duncan, and M. K. Sidhu, ""Episodic memory network connectivity in temporal lobe epilepsy," *Epilepsia*, vol. 63, no. 10, pp. 2597–2622, 2022.
- [25] A. J. Barnett, V. Man, and M. P. Mcandrews, "Parcellation of the Hippocampus Using Resting Functional Connectivity in Temporal Lobe Epilepsy," *Frontiers in Neurology*, 2019.